Draft version November 13, 2015
Preprint typeset using LaTeX style emulateapj v. 01/23/15

HCN 1-0 IS NOT A LINEAR TRACER OF DENSE GAS MASS IN THE GALACTIC CENTER

E.A.C. Mills[1]
University of Arizona Steward Observatory
Draft version November 13, 2015

ABSTRACT

We investigate the correlation of HCN 1-0 with dense gas mass in the Galactic center, inspired by the use of HCN 1-0 as a proxy for the amount of dense gas in extragalactic systems. We find that in the extreme environment of the Galactic center, on size scales up to those of individual giant molecular clouds, the HCN 1-0 luminosity is not correlated with the dense gas mass as measured from a Herschel column density map. The core of the massive cloud Sgr B2 with 10% of the total molecular gas mass in the Galactic center has less HCN 1-0 emission than clouds up to five times less massive due to self-absorption in this line, while several other clouds show an enhancement of HCN 1-0 by a factor of 2-3 relative to clouds of comparable mass. We do not perform a detailed comparison of infrared luminosity and HCN 1-0 luminosity, however we note that HCN 1-0 enhancements are not solely seen toward regions of strong infrared emission, and we suggest instead that shock chemistry may be the primary driver of enhanced HCN 1-0 emission. We also investigate other tracers having transitions near 3 mm, finding that HNC and HCO^+ largely behave like HCN, while HC_3N and CH_3CN are higher fidelity tracers of the amount of gas in denser clouds like Sgr B2. As HCN 1-0 appears to be both over- and under-luminous in individual Galactic center clouds, further study is necessary to assess the fidelity of HCN 1-0 as a tracer of gas mass in extreme environments and to determine which effect dominates in systems such as ULIRGs and high-redshift galaxies.

1. INTRODUCTION

While the history of the cosmic star formation rate is well known, peaking around a redshift of 1.9 (Madau et al. 1998; Madau & Dickinson 2014), the physics that drives the variation of the star formation rate with redshift, including its steep decline since a redshift of 2 (Behroozi et al. 2013; Moster et al. 2013), are still uncertain. In particular, there has been a lack of direct measurements of molecular gas mass and density over the same timescales to connect the star formation properties with the conditions in the gas reservoir. This lack of data is largely due to the difficulties of observing molecular gas, especially at large distances, which has previously limited observations to bright tracers of molecular gas (e.g., single lines of CO or HCN) that serve as proxies for (dense) gas mass. The bulk of these measurements have been limited to nearby systems (z <0.1 Gao & Solomon 2004a; Graciá-Carpio et al. 2008; Leroy et al. 2009; Saintonge et al. 2011; García-Burillo et al. 2012), though recently larger samples have begun to push out beyond a redshift of 1 (e.g., Gao et al. 2007; Tacconi et al. 2010, 2013; Saintonge et al. 2013; Carilli & Walter 2013; Genzel et al. 2015).

In the local universe, the use of CO as a gas tracer reveals a fundamental relationship between star formation (as traced by far-infrared luminosity) and gas surface density (Kennicutt 1998), although variations in the abundance and excitation of CO can change the CO to gas mass conversion factor (Sandstrom et al. 2013; Mashian et al. 2015). However, in massive, infrared-luminous galaxies, CO 1-0 is systematically weak compared to the far-infrared luminosity, and the Schmidt-Kennicutt relationship is not linear (Gao & Solomon 2004a). In contrast, HCN 1-0 retains a linear relationship with far-infrared luminosity over 7-8 orders of magnitude in infrared luminosity (The Gao-Solomon relation Gao & Solomon 2004b; Wu et al. 2005). The difference in behavior between HCN 1-0 and CO 1-0 in these systems can be explained if the HCN:CO ratio represents the fraction of dense (n $=10^4 - 10^5$ cm^{-3}) gas, which is suggested to be more fundamentally relevant for star formation (Lada et al. 2012).

In recent years the universal applicability of the Gao-Solomon relation to all extragalactic environments has been called into question. HCN 1-0 is observed to be anomalously bright in active galactic nuclei (AGN), compared to CO and HCO^+ (Davies et al. 2012; Imanishi et al. 2009; Kohno et al. 2003). Graciá-Carpio et al. (2006) also find that HCN 1-0 may be overluminous compared to HCO^+ in ultraluminous infrared galaxies (ULIRGs), and Privon et al. (2015) also find that overluminous HCN 1-0 is not limited to galaxies containing AGN. In addition to these indications that HCN 1-0 is overluminous in some environments, there are observations that a single power-law spectrum is insufficient to describe both normal galaxies and ULIRGs. Other studies have found that the Gao-Solomon relation becomes superlinear, with ULIRGs having a systematically higher (by a factor of 2-3) ratio of far-infrared luminosity compared to HCN 1-0, which is interpreted as increased star formation efficiency in these systems (Graciá-Carpio et al. 2008; García-Burillo et al. 2012). Gao et al. (2007) similarly found that their sample of high-redshift galaxies had systematically brighter L_{FIR} compared to HCN 1-0. It is standard to explain the variations in the HCN:IR ratio as differences in the star formation efficiency (or gas depletion time) as a function of environment, rather

bmills@aoc.nrao.edu
[1] E.A.C. Mills is a Jansky Fellow of the National Radio Astronomy Observatory, which is a facility of the National Science Foundation operated under cooperative agreement by Associated Universities, Inc..

than a failure of HCN 1-0 to trace the total dense gas mass (e.g., Juneau et al. 2009; Leroy et al. 2015; Usero et al. 2015).

However, there are several reasons that HCN 1-0 could fail to be a reliable tracer of the total dense gas mass in all environments. Although the modeling of Gao & Solomon (2004b) indicate that HCN 1-0 luminosity should be proportional to dense gas mass across a wide range of physical conditions, this assumes both a constant abundance, and purely collisional excitation. X-ray and photon-dominated regions are suggested to change the gas chemistry, increasing the abundance of HCN relative to other species (Lepp & Dalgarno 1996; Meijerink et al. 2007; Harada et al. 2013), while a strong 14 μm radiation field can induce radiative pumping in HCN, altering its level populations (Ziurys & Turner 1986; Aalto et al. 2007b; Sakamoto et al. 2010; Mills et al. 2013). Infrared pumping has also been suggested to induce weak masing in the 1-0 line (Matsushita et al. 2015), analogous to stronger masers observed in the envelopes of asymptotic giant branch stars (Olofsson et al. 1993; Izumiura et al. 1995). Although the optical thickness of HCN 1-0 (or CO 1-0) is suggested not to matter significantly, as extragalactic scaling relationships are often explained as counting optically thick (or thin) clouds, which as an ensemble are then proportional to the total mass (e.g. Wu et al. 2005), this assumption can break down: for example, when HCN is subject to self-absorption in very high column density environments like those in the nuclei of ULIRGs (Aalto et al. 2015).

To understand the relationship between the molecular gas supply and the peak and decline of the cosmic star formation rate, we need to be able to make accurate measurements of the gas mass out to high redshifts. To continue to use HCN 1-0 as a proxy for this mass, it necessary to understand any environmental dependencies on the fidelity of this tracer. In this paper we present the first resolved comparison of HCN 1-0 with an independent tracer of dense gas mass in an extreme environment: the Galactic center, a region with physical properties (high densities, temperatures, and turbulence) that are analogous to those in high-redshift galaxies (Kruijssen & Longmore 2013). We compare the HCN 1-0 luminosity in individual giant molecular clouds with the molecular gas mass from Herschel column density maps, and report on variations in the ratio of these two quantities: the dense gas conversion factor. We also compare the behavior of HCN 1-0 to that of other 3 mm tracers, including HCO^+ 1-0 and HC_3N 10-9. Finally, we discuss the implications of this study for the interpretation of past and future studies using HCN 1-0 as a tracer of dense gas in the extreme environments of luminous infrared galaxies and high-redshift systems.

2. DATA AND METHODS

Data for this analysis are taken from two sources. The first is a publicly-available 3 mm survey of the Galactic center with the 12 m Mopra telescope (Jones et al. 2012). These observations covered frequencies from 85.3 to 93.3 GHz, which in addition to HCN 1-0 includes observations of C_2H 1-0, c-C_3H_2 2_{12}-1_{01}, CH_3CN 5_K-4_K, CH_3CN 5_K-4_K, HC_3N 10-9, $HOCO^+$ 4_{04}-3_{03}, HNCO 4_{04}-3_{03}, HCO^+ 1-0, N_2H^+ 1-0, HNC 1-0, $HN^{13}C$ 1-0, $H^{13}CO^+$ 1-0, $H^{13}CN$ 1-0, ^{13}CS 2-1, SO 2_2-1_1, and SiO 2-1. The velocity resolution of these data is $\sim$2 km/s. The typical angular resolution of these data is 36″ which, at an assumed distance of 8.4 kpc to the Galactic center (Ghez et al. 2008), corresponds to a spatial resolution of 1.5 pc. The total extent of the mapped region spans 70 pc in Galactic latitude, and 370 pc in Galactic longitude. For the purposes of this analysis, we integrate the data cubes for each line over a velocity range [-230 km s^{-1},+230km s^{-1}] sufficient to include all CMZ gas, discarding emission below a conservative 5-sigma cut off ($\sim$0.34 K km s^{-1}) for the lines with more prominent spurious features (HCN, HCO^+, HNC, $H^{13}CN$, HNCO, and HC_3N; see discussion in Jones et al.), and a smaller cut of 3-sigma (0.2 K km s^{-1}) for the remaining, primarily weaker lines. This is sufficient to eliminate the effects of artifacts such as anomalous baseline shapes in all but the weakest lines (e.g., C_2H, c-C_3H_2). Following Jones et al. (2012), we do not correct for the main beam efficiency of Mopra, which for the extended emission in these maps will be $\sim$0.65 (as measured at 86 GHz by Ladd et al. 2005) and variable with frequency. Line luminosities in this paper are then given in intrinsic units of uncorrected antenna temperature (T_A*) rather than main beam temperature. The resulting integrated intensity map of HCN 1-0 is shown in Figure 1.

The second source of data is an H_2 column density map (Battersby et al. in prep), which is derived from measurements of the submillimeter dust emission made with Herschel Hi-Gal in the Galactic center (Figure 1, Molinari et al. 2011). The map is based on the algorithm presented in Battersby et al. (2011) for Galactic plane data. The resolution of the resulting column density map is 36″, identical to the resolution of the MOPRA data. Note that data is lacking from the central pixels of the brightest submillimeter source, Sgr B2, because the emission in these pixels is saturated. As a result, these pixels are masked, and the total mass of Sgr B2 will be underestimated.

As the molecular line and column density maps have identical resolution, the first step is to identically pixelize the maps. Ratio maps are then constructed, representing the correspondence between the luminosity of each line and the dense gas mass, which is proportional to the H_2 column density at each position. Only those pixels in all maps that have an H_2 column density above a chosen threshold ($N(H_2) = 7\times10^{22}$ cm $^{-2}$) are retained in the main analysis; this threshold is selected in order to isolate the emission from the most massive cloud cores, and the resulting thresholded ratio maps are shown in Figure 2.

We employ two methods for comparing the variations in the ratio of HCN 1-0 luminosity and $N(H_2)$: first, we plot the total HCN 1-0 luminosity and the total mass of H_2 in Figure 3 for a sample of 14 giant molecular cloud cores: GCM1.6-0.03, Sgr D, GCM0.83-0.18 (a ring of gas and dust to the southwest of Sgr B2), Sgr B2 – both its dense core (R$\sim$15 pc) and its 'halo' (R$\sim$50 pc), GCM0.50+0.00 (the easternmost cloud in the dust ridge, near Sgr B1), the remaining dust ridge clouds, GCM0.25+0.01 (the 'Brick'), GCM0.11-0.08 (together with two other neighboring clouds to the east of the 50 km s^{-1} cloud), GCM0.07+0.04 (A cloud on the edge of the Arched filaments), GCM-0.02-0.07 (the 50 km s^{-1} cloud), GCM-0.13-0.08 (the 20 km s^{-1} cloud), and Sgr

C. The locations of these clouds are shown in the first subplot of Figure 2. In choosing to focus this analysis on the cores of these clouds above a given column density, the goal is to ensure that HCN 1-0 luminosity is primarily being compared just to the mass of dense gas in the Galactic center. While the column density should in principle be sensitive to the mass of gas at any density, the cores of these clouds are believed to have average densities $> 10^4$ cm^{-3} (Güsten & Henkel 1983; Zylka et al. 1992; Serabyn et al. 1992; Longmore et al. 2012, 2013).

Note that the line luminosity and the column density are integrated over a region in the cloud above a given column density threshold, so the masses given here are equivalent to the mass of a subset of the cloud core, and are not equivalent to the total cloud masses. The column density thresholds used are 2×10^{23} cm^{-2} for the core of Sgr B2 and GCM0.50+0.00, in order to separate them from the surrounding cloud 'halo', and 7×10^{22} cm^{-2} for all other clouds. The 'halo' of Sgr B2 is defined by gas above this column density threshold over the entire contiguous Sgr B2 complex, but excluding the two cores (Sgr B2 and GCM0.50+0.00) where the column density is larger than 1.5×10^{23} cm^{-2}. This threshold is chosen so that the mass of the Sgr B2 core and halo are roughly equivalent. Total masses are then calculated from the integrated H_2 column density according to the formula:

$$M_{\rm H2} = \mu_{\rm H2}\, m_{\rm H} \int N_{\rm H2}\, dA \qquad (1)$$

where $\mu_{\rm H2}$ is the mean molecular weight of the gas, $m_{\rm H}$ is the mass of a Hydrogen atom, and $\int N_{\rm H2}\, dA$ is the column density of H_2 (in cm^{-2} integrated over the area of the cloud (in cm^2).

Second, we construct plots of the pixel-by-pixel variations (shown in Figure 4) in which the line luminosity of each pixel is plotted against N(H_2). To aid in the interpretation of these plots we additionally colorize points if they correspond to one of the thirteen selected clouds. Identical plots of the pixel values for all of the mapped 3 mm lines are also shown in Figure 4. Note that the mass of the Sgr B2 core is plotted as a lower limit, as the column density of the central, saturated pixels is not included in the total integrated mass.

3. RESULTS

The main finding of this paper shown in Figure 3 is that the luminosity of HCN 1-0 is not directly proportional to the mass of dense H_2 in the Galactic center. The core of Sgr B2 is underluminous, having an integrated line intensity equivalent to that of clouds up to five times less massive. It also has five times weaker HCN 1-0 than the halo of the Sgr B2 cloud which contains a roughly equivalent mass of dense gas. Additionally, GCM-0.02-0.07 and GCM0.11-0.08 have integrated line intensities 3 times brighter than other clouds of comparable mass. This indicates that the conversion factor from HCN 1-0 to total dense gas mass is subject to significant variation in the environment of the Galactic center.

Examining Figure 4, which shows the distribution of line luminosity and N(H_2) for individual pixels in each cloud, it is clear that a similar behavior (underluminous line emission in the core of Sgr B2, and overluminous emission in GCM-0.02-0.07 and/or GCM0.11-0.08) is also seen for $H^{13}CN$, HCO^+, HNC, SiO, and N_2H^+. All of these molecules show clear non-monotonic behavior, which often includes a bifurcation around a column density of log(N) = 23.0-23.5. However, for a subset of other molecules which are either hot-core molecules (CH_3CN, CH_3CN, SO) or trace more highly-excited gas ($HOCO^+$, HNCO, HC_3N), line brightness increases roughly monotonically with column density. Finally, we also show the distributions of pixel values for other molecules which show no clear pattern: these molecules include tracers often used to probe photodissociation regions (C_2H, c-C_3H_2), and weak isotopologues ($H^{13}CO^+$, $HN^{13}C$, ^{13}CS). It is notable that in the majority of tracers, GCM-0.02-0.7 is overluminous compared to other clouds having a similar distribution of column densities.

Finally, while we have focused our analysis on the cores of well-known clouds which should be representative of the densest gas in the Galactic center, only 32% of the total gas mass in the Galactic center as traced by the column density map lies above the chosen column density threshold of N(H_2) = 7×10^{22} cm $^{-2}$. We therefore also investigate the behavior of the more diffuse or extended component in HCN 1-0. The ratio of HCN 1-0 luminosity to the column density above a threshold of 1×10^{22} cm $^{-2}$ is shown in Figure 5. The ratio varies by more than two orders of magnitude: it reaches a minimum of *sim*0.5 (the units on this ratio are K km s^{-1} per 10^{22} cm^{-2}) in Sgr B2, and maxima of $\sim$ 60 are reached in the gas infrared bubble (Rodríguez-Fernández et al. 2001) and north of Sgr D. These extended regions have ratios more than 3× greater than those found in any of the cloud cores. Overall, a weak trend is seen that HCN 1-0 is brighter in the lower column density gas: 80% of the HCN 1-0 emission comes from gas with column density less than 7×10^{22} cm $^{-2}$, accounting for 68% of the total mass, while only 20% of the HCN 1-0 comes from gas with column density above 7×10^{22} cm $^{-2}$, accounting for 32% of the total gas mass.

4. DISCUSSION

4.1. *Why is HCN 1-0 underluminous in Sgr B2?*

The most surprising result of this analysis is the relative weakness of 3 mm line emission from the core of Sgr B2, the most massive molecular cloud in the Galactic center. Here, we investigate several scenarios to account for the observed weakness of HCN 1-0 and other lines.

We first examine whether the observed weakness of HCN 1-0 in the Sgr B2 core could actually be a results of overbrightness of the far-infrared dust continuum in the Herschel bands. As seen in Molinari et al. (2011), the dust temperatures in the core of Sgr B2 are not globally elevated over the values seen in other clouds, so although there is local hot dust near the embedded HII regions, it does not appear that this would significantly change the inferred column density and mass of this source. If there is a variation in the dust emissivity properties, it would be necessary to explain why this is confined just to this single cloud in the Galactic center. However, the strongest argument against a difference in the dust properties leading to an overestimated mass is that the approximate mass of Sgr B2 complex estimated from the dust continuum (a few 10^6 $M_\odot$) is consistent with that

determined using optically-thin measurements of $C^{18}O$ (Dahmen et al. 1998).

As noted by (Gao & Solomon 2004a), the brightness of HCN 1-0, which has a critical density of $\sim 10^5$ cm^{-3}, should be a good tracer of total gas over a large range of gas densities. Using RADEX, we find that for a constant column density, line width, and a temperature of 100 K, the intensity of HCN 1-0 should vary by less than a factor of 2 for volume densities ranging from n = $10^5 - 10^7$ cm^{-3}. Even at n = 10^8 cm^{-3}, higher than densities previously measured in Sgr B2 (Lis & Goldsmith 1991; Etxaluze et al. 2013), HCN 1-0 should only be a factor of 3 fainter than at n = 10^5 cm^{-3}. Varying the temperature from 50 to 200 K and holding all other parameters fixed also only changes the intensity of HCN 1-0 by at most a factor of 3. However, if the gas density were as low as n = 10^4 cm^{-3}, the brightness of HCN 1-0 could be almost an order of magnitude lower, consistent with what is observed. This explanation is problematic, as it requires that the observed high column density of the core of Sgr B2 be due to the projection of a large column of very low volume density gas. Although Sgr B2 is located at a tangent point of many orbital models of the Galactic center (Molinari et al. 2011; Kruijssen et al. 2015) where there could be confusion with the projection of gas over a range of distances, such low densities would be surprising, especially as the measured ratio of HCN 1-0 to N(H_2) is lowest toward the center of Sgr B2, where there are reliable measurements of extremely large volume densities on individual cores (n=10^7 cm^{-3} Lis & Goldsmith 1991). We suggest that this then an unlikely explanation, although it illustrates a need for improved studies of the density of the entire Sgr B2 complex.

We also consider whether HCN could have a lower abundance in Sgr B2 than in other clouds in the Galactic center. Sgr B2 is likely unique in several ways: in addition to being the most massive cloud by an order of magnitude, it has a higher average density than other Galactic center clouds (Lis & Goldsmith 1991; Güsten & Henkel 1983), and potentially a higher temperature as well (Hüttemeister et al. 1993; Hüttemeister et al. 1995; Etxaluze et al. 2013; Mills & Morris 2013; Ginsburg et al. 2015). It also has by far the most active ongoing embedded star formation of any Galactic center cloud (Vogel et al. 1987; Gaume & Claussen 1990; de Pree et al. 1998) and hosts one of the most chemically-rich high mass protostellar sources in the Galaxy (e.g. Snyder et al. 1994; Miao et al. 1995). One possibility is that Sgr B2, having the most active internal star formation of any Galactic center cloud, is subject to a stronger internal UV radiation field that is more efficiently photodissociating HCN and similar molecules in the denser gas at the center of this cloud. However, this explanation seems unlikely given that the high column densities should shield most of the gas from these effects and HC_3N, which is more easily photodissociated (Martín et al. 2012), is not underabundant in Sgr B2 compared to other Galactic center clouds.

Given the extremely high column densities of Sgr B2 (Qin et al. 2011, peak column densities $> 10^{25}$ cm^{-2}[), we also investigate whether the weakness of HCN 1-0 could occur due to optical thickness in this line. In addition to HCN 1-0, we also observed $H^{13}CN$, which should be $\sim$ 25 times less abundant than $H^{12}CN$ (Wilson & Rood 1994; Wilson 1999; Riquelme et al. 2010). We find that $H^{12}CN/H^{13}CN$ is $\sim$15-25 in Sgr B2, which would indicate that this line is largely optically thin (in contrast, $H^{12}CN/H^{13}CN$ ranges from 5-6 in GCM-0.02-0.07 and GCM-0.13-0.08, indicating that HCN 1-0 in these clouds is optically thick). Further, $HC^{15}N$, which should be 8-12 times weaker than $H^{13}CN$ based on the $^{14}N/^{15}N$ ratio in this source (D. Halfen and A. Belloche, Private communication) is not detected in Sgr B2 at all (Jones et al. 2008).

However, examining the spectra of all detected transitions toward the core of Sgr B2 (Figure 6), a similar but distinct effect is noted: the shape of many transitions have a two-peaked structure, with a pronounced dip at the central velocity of Sgr B2. While a difference in the shape of the spectra could be due to spatial variations in abundance, the symmetry of the two peaks around the central velocity is a clear signature of self absorption. In self absorption, cooler or lower-excitation gas is present along the line of sight and at the same velocity as warmer or higher-excitation gas. The foreground column of cooler molecules then absorbs the emission signature from the more excited background molecules. As would be expected for self absorption, the transitions which are most affected are the lowest-J transitions: All species whose 1-0 transition is observed (HCN,HCO^+,HNC, including the ^{13}C isotopologues of these species, C_2H and N_2H^+) exhibit this dip. The dip is also seen in the 2-1 transitions of ^{13}CS, SiO, and c-C_3H_2 though not in the 2_2-1_1 line of SO. However, it is not present in $HOCO^+$, CH_3CN, CH_3CN, HC_3N, or HNCO, all of which are observed in transitions having $J_{up} \geq 4$. We thus favor self absorption as the cause of the apparently weak emission of HCN 1-0 in Sgr B2. While a lesser degree of self-absorption is seen in the spectra of HCN 1-0 toward GCM1.6-0.03, GCM-0.13-0.08, and Sgr C, none of these sources also have self-absorption in $H^{13}CN$.

Unlike a pure optical depth effect, where less abundant isotopologues should be proportionately stronger and thus better tracers of the high column density gas, here, the observed isotopologues of all species appear similarly self-absorbed in the core of Sgr B2. In fact, we cannot entirely rule out that HCN and even $H^{13}CN$ are also optically-thick, as the nondetection of $HC^{15}N$ 1-0 could indicate that it also is self-absorbed, but we reiterate that optical depth alone is not the cause of the apparent underluminosity of the Sgr B2 core in HCN 1-0. Self-absorption in higher-J lines of HCN and HCO^+ has also been observed in the Galactic center 'Circumnuclear Disk' surrounding the supermassive black hole, however here only the ^{12}C lines are self-absorbed (Mills et al. 2013). The observed self absorption of even the ^{13}C isotopologues toward the Sgr B2 core then likely requires a higher column of self-absorbing gas toward this source. Given that the self-absorption happens at the same velocity as the peak emission in the Sgr B2 core, it is likely that this is a fairly localized effect (i.e., this is not a resulting of intervening, foreground gas in the Galactic disk). It is possible that the self-absorption signature is due to very local gas: for example, as a signature of infall or outflow. Infalling gas might be expected to show a stronger blueshifted or negative velocity peak (a reverse

P-Cygni profile), while outflowing gas would show the opposite signature. No consistent signature is seen toward the Sgr B2 core: the strongest (and likely most optically-thick) lines have a signature that could be interpreted as outflow, while the isotopologues have a signature that could be more consistent with infall. Higher-excitation lines of HCN toward the Sgr B2 (M) hot core have previously been used to infer the opposite effect: a signature of infall is seen in more optically thick and lower-excitation lines, and a reversal of infall in the more optically-thin and higher-excitation lines. However, with the low resolution of our observations, it is not possible to make any definitive claims regarding the dynamics of this complicated region. We note that independent of the observed self-absorption there is also likely absorption against the embedded HII regions in Sgr B2 – however, as these HII regions are more centrally concentrated than the self-absorption signature, and there are molecules for which dip is not seen, we do not believe the observed signature can be due to absorption against HII regions alone.

The fact that the core of Sgr B2, the most massive and dense cloud in the Galactic center is underluminous in HCN 1-0 has important implications, as it is often taken to be a template for conditions that are widespread in more extreme starbursts or high-redshift systems. This result indicates that caution should be taken when interpreting variations of the ratio of HCN 1-0 to far-infrared luminosity in extreme systems, as they could instead be due in whole or in part to HCN 1-0 underestimating the total dense gas mass. We discuss this further in Section 4.3.

4.2. *What is the mechanism behind overluminous HCN 1-0 in Galactic center clouds?*

Outside of the Sgr B2 core, three dense clouds: GCM-0.02-0.07, GCM0.07+0.04, and GCM0.11-0.08, have brighter HCN 1-0 emission by a factor of ∼3 than other clouds of comparable mass. All of these clouds are near each other, projected within 30 pc of the supermassive black hole. Before assuming that HCN 1-0 is overluminous in these clouds, we ask whether these could instead be regions where the conversion factor between HCN 1-0 and the (dense) gas mass is "normal" and not reduced due to the same processes (which we suggest are chemical depletion) that are responsible for the relative weakness of this line in the Sgr B2 core. For this to be the case, the clouds with less HCN 1-0 emission than these three clouds would have to be those with the most similar chemical and physical environment to the Sgr B2 core. However, most of those clouds (e.g., GCM0.25+0.01, GCM0.13+0.08) are not actively forming stars, and they are not suggested to be denser or warmer than clouds having proportionately higher HCN 1-0 luminosity (GCM-0.02-0.07), so there is no clear reason to believe them to be more similar to the Sgr B2 core. Further, comparison with $H^{13}CN$ shows that clouds with faint HCN 1-0 are not preferentially optically thick, nor do they (apart from the Sgr B2 core) exhibit signatures of self-absorption, so it also does not appear that variations in HCN 1-0 luminosity can be explained by optical depth. In fact GCM-0.02-0.07, which has some of the brightest HCN 1-0 emission, has an $H^{12}CN/H^{13}CN$ ratio of 5, indicating a moderate optical depth, and compared to GCM0.25+0.01 which has a comparable mass, it is actually 10 times brighter in $H^{13}CN$ 1-0. GCM-0.13-0.18 is similarly optically thick. For now, we therefore assume that the HCN 1-0 observed in these three clouds is overluminous (and that although GCM-0.13-0.08 does not appear overluminous for its mass, this is only due to the optical thickness of the HCN 1-0 line in this source).

Similar to Sgr B2, we first ask whether this difference could be due to varying excitation conditions for HCN 1-0. Other studies have shown that there is no significant difference in the kinetic temperature (Hüttemeister et al. 1993; Ao et al. 2013; Mills & Morris 2013; Ginsburg et al. 2015) or line width (Jones et al. 2012) between the clouds in our study with weak and bright HCN 1-0. Our RADEX analysis then indicates that for a constant column density, variations in volume density from $n=10^5 - 10^7$ should change the line brightness by less than a factor of 2, the observed overluminosity can only be explained if the three bright clouds are the only clouds (apart from the Sgr B2 core) with $n > 10^{4.5}$ cm^{-3}. Independent studies of cloud densities (Serabyn et al. 1992; Longmore et al. 2013; Güsten & Henkel 1983; Zylka et al. 1992) are inconsistent with this scenario, and in fact even higher ratios of HCN 1-0 to $N(H_2)$ are seen in the more extended gas which is likely to be at yet lower densities. There could still be excitation differences due to radiative excitation or masing, however for either of these to be applicable, HCN 1-0 should be well correlated with IR.

We next ask whether the variations in the HCN 1-0 luminosity could be consistent with a dependency of this quantity on the environment. It has been suggested that overluminous HCN could be due to X-ray chemistry (Lepp & Dalgarno 1996; Meijerink et al. 2007; Harada et al. 2013). While several regions of enhanced emission are associated with X-ray sources (GCM-0.02-0.07 borders a supernova remnant, and clouds in the GCM0.11-0.08 complex are observed to have a propagating X-ray light echo Ponti et al. 2010) that may also be related to enhanced SiO in these regions (Martín-Pintado et al. 2000), there is no X-ray source associated with the bright HCN 1-0 north of Sgr D (Ponti et al. 2015). We also investigate whether, specifically, the enhanced HCN 1-0 is correlated with infrared emission. The three clouds with highest HCN 1-0 (G0.07+0.04, GCM0.11-0.08, and GCM-0.02-0.07) are projected against the infrared bubble. While this might suggest a connection between HCN 1-0 and the presence of a strong external IR field, the region north of Sgr D has extremely elevated HCN 1-0 in Figure 5 without significant IR emission. We also note that although Sgr B2 has both a strong internal infrared field from embedded formation and a recent X-ray light echo observed to be propagating through the cloud (Terrier et al. 2010), self absorption prevents us from determining whether HCN 1-0 is enhanced in the Sgr B2 core.

One remaining possibility is that HCN 1-0 is preferentially enhanced in some clouds and regions of the Galactic center due to elevated shock activity. HCN abundances have been observed to be enhanced by 1-2 orders of magnitude in shocked environments ranging from protostellar outflows to extragalactic outflows (Jørgensen et al. 2004; Tafalla et al. 2010; Aalto et al. 2015). GCM-0.02-0.07 borders a supernova remnant and shows multiple signs that it is experiencing shocks from this interactions

(Sjouwerman et al. 2010; Yusef-Zadeh et al. 1996), and while the GCM0.11-0.08 complex is not suggested to be interacting with a supernova remnant or to have undergone a cloud collision, it could be possible to explain enhanced shock activity in these clouds due to interaction with the expanding IR bubble, or as a result of their recent pericenter passage in the model of Kruijssen et al. (2015). Importantly, the enhanced HCN 1-0 emission north of Sgr D is also coincident with SiO emission, which is often indicative of shock chemistry (Martin-Pintado et al. 1997). As Sgr B2 has been suggested to have undergone a cloud-cloud collision, this cloud might also be expected to host enhanced shock activity– and indeed, it is possible that in the Sgr B2-halo, which is largely free of self-absorption, that the HCN 1-0 line is overbright (SiO and HNCO, another shock tracer, both appear to be strong and perhaps overluminous in this region as well). Additional work is needed to confirm this hypothesis: for example, shocks might be expected to correspond with regions of increased turbulence that could manifest as increased line widths. Enhanced emission from other shock tracers could also be searched for, such as the 36 GHz methanol maser, which has been recently observed to be widespread in the Galactic center (Yusef-Zadeh et al. 2013; Mills et al. 2015).

While the observed overluminosity of HCN 1-0 in several Galactic center clouds is small (on the order of a factor of 3), determining the mechanism that is responsible is important for assessing whether this effect might become more pronounced in other environments. Identifying the mechanism which is leading to enhanced HCN 1-0 can also give insight into additional diagnostics which should be performed in order to assess whether HCN 1-0 is accurately representing the total dense gas mass in a given environment.

4.3. *Implications of a varying HCN 1-0 to dense gas mass conversion factor for the Gao-Solomon relation*

The Gao-Solomon relation shows that HCN 1-0, which is assumed to be proportional to the amount of dense gas, is tightly correlated with the far infrared luminosity over 10 orders of magnitude in IR brightness (Gao & Solomon 2004b; Wu et al. 2005). Wu et al. (2005) interpret this as indicating that individual, sub-parsec scale dense cores are the fundamental unit of dense gas mass associated with star formation, and that the Gao Solomon relation on larger scales is essentially counting the number of these structures. Here, we find that, at least in the extreme environment of the Galactic center, the HCN 1-0 luminosity cannot be assumed to be proportional to the amount of dense gas on size scales at or smaller than a molecular cloud (We will investigate the correlation of HCN 1-0 with IR in the Galactic center in a future paper).

However, at least in the center of our Galaxy, it is not clear that the observed over and under-luminosity of HCN 1-0 would contribute to a strong global deviation from the Gao-Solomon law. Although the Sgr B2 core has HCN 1-0 emission consistent with a cloud $\sim$5 times less massive, this missing luminosity would only result in missing $\lesssim 10\%$ of the total mass of dense gas in the Galactic center, some of which would be balanced out by the "extra mass" inferred from overbright HCN 1-0 in other clouds. However, because the HCN 1-0 luminosity does not increase monotonically with dense gas mass, this suggests that global variations in the environment or gas properties of other galaxies could lead to systematic errors when interpreting HCN 1-0 as proportional to the total mass of dense gas in more extreme extragalactic environments.

Certain environments in particular should be more prone to the self-absorption in HCN 1-0 observed toward the Sgr B2 core. In clouds having an excitation gradient that increases radially toward the center, one might expect to see self-absorption in the lower J levels of a given common gas tracer. Such excitation gradients would be typical of clouds with embedded active star formation (as in Sgr B2), or embedded AGN, as is has recently been noted in a number of compact sources of nuclear emission (Aalto et al. 2015). Self-absorption could also occur in cases where there are strong global signatures of outflow or infall. Self absorption also might be expected to depend on the relative orientation of a warm background source and cool foreground emission, but as it requires the foreground and background gas to be at the same velocity, it should not be a general feature of galaxy disks observed edge-on (for example, we note that self-absorption is only seen for a small number of the surveyed Galactic center clouds, though all are observed through edge-on disk of our own Galaxy).

In general, the results of this paper do not indicate a broad failure of the interpretation of the Gao-Solomon relation as indicating that the amount of dense gas is proportional to the amount of star formation, at least in environments such as the disk of our Galaxy and other normal galaxies. Instead, we suggest that observed deviations from the Gao Solomon relation in extreme environments (e.g., those of ULIRGS, high redshift galaxies, and AGN) should be carefully examined for a failure of HCN 1-0 to trace the true quantity of dense gas present before assuming a physical explanation such as a shorter gas depletion time (e.g., García-Burillo et al. 2012; Juneau et al. 2009; Leroy et al. 2015; Usero et al. 2015). Such studies will also be important for determining whether the Galactic center conditions responsible for variations in the HCN 1-0 to dense gas conversion factor are actually relevant for other galaxies, or whether deviations from the Gao-Solomon relation in other systems are due to entirely separate effects that are a result of environments that are not sampled in our own Galaxy.

4.4. *Other lines*

By analyzing the other 3 mm lines, we also are able to comment on tracers which are better representative of the proportionately large mass of the core of the Sgr B2 cloud. We suggest that HC_3N and CH_3CN are relatively strong, and appear, at least in the Galactic center, to obey a more monotonic scaling relationship between their brightness and the total dense gas mass. We suggest that these tracers largely succeed where HCN and similar tracers fail due to being unaffected by self-absorption: both of these species have a chemistry more typical of hot-core molecules that are somewhat less likely to be seen in cooler cloud envelopes, they have lower abundances, and are higher-excitation ($J_{up} \geq 4$) transitions with higher critical densities. Although HNCO shares many of these qualities, it is more complicated: while

Figure 4 may indicate that HNCO also has a monotonic relationship with dense gas mass, Figure 3 shows that the Sgr B2 core is still underluminous in this line compared to the Sgr B2 halo. Unlike other tracers where the Sgr B2 core appears underluminous, it does not appear that HNCO shows signatures of self absorption in its spectrum toward the Sgr B2 core, However, as HNCO is suggested to behave like a shock tracer in some environments (e.g., Meier & Turner 2005), it may be that this tracer is actually overluminous in regions like the Sgr B2 halo. Either way, this behavior makes it an unreliable indicator of total dense gas mass.

Higher-excitation tracers of more common molecules are also likely to be less affected by self-absorption. For example, in observations of the Galactic center circumnuclear disk while self-absorption is seen in the J = 3-2 and 4-3 lines of HCN, self absorption is no longer present in the 8-7 line (Mills et al. 2013). This could make diatomic tracers of dense gas such as CS a more optimal tracer in a given band, as they will have higher-J transitions than HCN, HNC, or HCO^+at similar frequencies. In the observations analysed here, the 2-1 transition of ^{13}CS can be seen in Figure 6 to have less self absorption than the 1-0 transitions of $H^{13}CN$, $HN^{13}C$, and $H^{13}CO^+$. However, care should still be taken in avoiding tracers subject to self-absorption to also avoid tracers such as SiO that are known to be enhanced by shocks.

In general, caution should be taken in using any single transition to represent total mass: although HC_3N is a better tracer of the total mass of the Sgr B2 core, GCM-0.02-0.07 is still overluminous in HC_3N (possibly because this cloud has an extremely high abundance of C^+ Tanaka et al. 2011), and HC_3N has been observed to be enhanced in active nuclei (Aalto et al. 2007a). We suggest that these alternative tracers are better used not on their own, but to augment a more abundant tracer such as HCN 1-0, to guard against the underestimation of the dense gas mass due to the effects of self-absorption. Further study of the correspondence of HCN with shocks in extreme extragalactic environments should also be made to determine whether similar tracers like HNC, HCO^+, or CS are less affected and thus more suitable.

Finally, we note that this study is based upon the assumption that the submillimeter dust emission traced by Herschel is a high-fidelity tracer of the total gas column density (and thus mass) in the Galactic center. This appears to be a good assumption in less-extreme environments (e.g. Battersby et al. 2014). Bulk dust properties have also been shown to be extremely similar in environments ranging from our Galaxy to nearby normal star forming galaxies and submillimeter galaxies (Scoville et al. 2014). We find that the dust-derived cloud masses of this study are broadly consistent with cloud masses previously inferred using $C^{18}O$ (Dahmen et al. 1998), however, this assumption (e.g., that the dust to gas ratio does not significantly vary as a function of environment) has yet to be carefully tested in the Galactic center, or investigated on smaller spatial scales than this study. However, despite this remaining uncertainty we do not believe that the use of dust emission to determine masses affects the results of this paper.

5. CONCLUSIONS

Below, we summarize the main findings of this paper:

- In the Galactic center HCN 1-0 luminosity does not increase monotonically with increasing dense gas mass, on the scale of individual giant molecular cloud cores.
- The core of Sgr B2 has an HCN 1-0 luminosity equivalent to clouds having five times less mass. The faintness of this line appears to be a result of self-absorption in this source. Based on this, we caution against the interpretation of increased L_{FIR}/HCN 1-0 as indicative of a higher star formation efficiency or lower gas depletion time in extreme environments that might be dominated by sources like embedded starbursts or AGN having a similar excitation gradient, with more highly-excited gas surrounded by a lower-excitation envelope.
- Several cloud cores, all located in the central 30 parsecs, have ∼3 times brighter HCN 1-0 than other clouds of similar mass. We also find several contiguous regions of extended gas that have 3-10 times more luminous HCN 1-0 per unit $N(H_2)$ than in any of the cloud cores studied here. We suggest that increased HCN 1-0 luminosity could be due to enhanced shock activity.
- In order to avoid biases in the inferred gas mass due to the systematic under- or over-luminosity of a given tracer, we recommend that observations of standard tracers such as HCN 1-0 or CO 1-0 be supplemented with observations of higher-excitation or hot-core tracers, and that tracers whose abundances are known to be most strongly affected by shocks, such as SiO and HNCO, be avoided.

ACKNOWLEDGEMENTS

The author thanks Cara Battersby for kindly sharing the Herschel column density map before publication. The author also thanks Jonathan Henshaw, Steven Longmore, David Meier, Susanne Aalto, and George Privon for useful discussion and suggestions that significantly improved the paper.

REFERENCES

Aalto, S., Monje, R., & Martín, S. 2007a, A&A, 475, 479
Aalto, S., Spaans, M., Wiedner, M. C., & Hüttemeister, S. 2007b, A&A, 464, 193
Aalto, S., Garcia-Burillo, S., Muller, S., et al. 2015, A&A, 574, A85
Aalto, S., Costagliola, S. M. F., Gonzalez-Alfonso, E., et al. 2015, arXiv.org, 1504.06824v1
Ao, Y., Henkel, C., Menten, K. M., et al. 2013, A&A, 550, A135
Battersby, C., Bally, J., Dunham, M., et al. 2014, ApJ, 786, 116
Battersby, C., Bally, J., Ginsburg, A., et al. 2011, A&A, 535, A128
Behroozi, P. S., Wechsler, R. H., & Conroy, C. 2013, ApJ, 770, 57
Carilli, C. L., & Walter, F. 2013, ARA&A, 51, 105

Dahmen, G., Huttemeister, S., Wilson, T. L., & Mauersberger, R. 1998, A&A, 331, 959
Davies, R., Mark, D., & Sternberg, A. 2012, A&A, 537, A133
de Pree, C. G., Goss, W. M., & Gaume, R. A. 1998, Astrophysical Journal v.500, 500, 847
Etxaluze, M., Goicoechea, J. R., Cernicharo, J., et al. 2013, A&A, 556, A137
Gao, Y., Carilli, C. L., Solomon, P. M., & Vanden Bout, P. A. 2007, The Astrophysical Journal, 660, L93
Gao, Y., & Solomon, P. M. 2004a, The Astrophysical Journal Supplement Series, 152, 63
—. 2004b, The Astrophysical Journal, 606, 271
García-Burillo, S., Usero, A., Alonso-Herrero, A., et al. 2012, A&A, 539, A8
Gaume, R. A., & Claussen, M. J. 1990, Astrophysical Journal, 351, 538
Genzel, R., Tacconi, L. J., Lutz, D., et al. 2015, ApJ, 800, 20
Ghez, A. M., et al. 2008, ApJ, 689, 1044
Ginsburg, A., Henkel, C., Ao, Y., et al. 2015, ArXiv e-prints, arXiv:1509.01583
Graciá-Carpio, J., Garcia-Burillo, S., Planesas, P., & Colina, L. 2006, The Astrophysical Journal, 640, L135
Graciá-Carpio, J., García-Burillo, S., Planesas, P., Fuente, A., & Usero, A. 2008, A&A, 479, 703
Güsten, R., & Henkel, C. 1983, A&A, 125, 136
Harada, N., Thompson, T. A., & Herbst, E. 2013, ApJ, 765, 108
Hüttemeister, S., Wilson, T. L., Bania, T. M., & Martin-Pintado, J. 1993, Astronomy and Astrophysics (ISSN 0004-6361), 280, 255
Hüttemeister, S., Wilson, T. L., Mauersberger, R., et al. 1995, Astronomy and Astrophysics (ISSN 0004-6361), 294, 667
Imanishi, M., Nakanishi, K., Tamura, Y., & Peng, C.-H. 2009, AJ, 137, 3581
Izumiura, H., Ukita, N., & Tsuji, T. 1995, ApJ, 440, 728
Jones, P. A., Burton, M. G., Cunningham, M. R., et al. 2008, Monthly Notices of the Royal Astronomical Society, 386, 117
Jones, P. A., Burton, M. G., Cunningham, M. R., et al. 2012, MNRAS, 419, 2961
Jørgensen, J. K., Hogerheijde, M. R., Blake, G. A., et al. 2004, A&A, 415, 1021
Juneau, S., Narayanan, D. T., Moustakas, J., et al. 2009, ApJ, 707, 1217
Kennicutt, Jr., R. C. 1998, ApJ, 498, 541
Kohno, K., Ishizuki, S., Matsushita, S., Vila-Vilaró, B., & Kawabe, R. 2003, PASJ, 55, L1
Kruijssen, J. M. D., Dale, J. E., & Longmore, S. N. 2015, MNRAS, 447, 1059
Kruijssen, J. M. D., & Longmore, S. N. 2013, MNRAS, 435, 2598
Lada, C. J., Forbrich, J., Lombardi, M., & Alves, J. F. 2012, The Astrophysical Journal, 745, 190
Ladd, N., Purcell, C., Wong, T., & Robertson, S. 2005, PASA, 22, 62
Lepp, S., & Dalgarno, A. 1996, A&A, 306, L21
Leroy, A. K., Walter, F., Bigiel, F., et al. 2009, AJ, 137, 4670
Leroy, A. K., Bolatto, A. D., Ostriker, E. C., et al. 2015, ApJ, 801, 25
Lis, D. C., & Goldsmith, P. F. 1991, Astrophysical Journal, 369, 157
Longmore, S. N., Rathborne, J., Bastian, N., et al. 2012, ApJ, 746, 117
Longmore, S. N., Kruijssen, J. M. D., Bally, J., et al. 2013, ArXiv e-prints, arXiv:1304.2397
Madau, P., & Dickinson, M. 2014, ARA&A, 52, 415
Madau, P., Pozzetti, L., & Dickinson, M. 1998, The Astrophysical Journal, 498, 106
Martín, S., Martín-Pintado, J., Montero-Castaño, M., Ho, P. T. P., & Blundell, R. 2012, A&A, 539, A29
Martin-Pintado, J., de Vicente, P., Fuente, A., & Planesas, P. 1997, ApJ, 482, L45+
Martín-Pintado, J., de Vicente, P., Rodríguez-Fernández, N. J., Fuente, A., & Planesas, P. 2000, A&A, 356, L5
Mashian, N., Sturm, E., Sternberg, A., et al. 2015, ApJ, 802, 81
Matsushita, S., Trung, D.-V., Boone, F., et al. 2015, ApJ, 799, 26
Meier, D. S., & Turner, J. L. 2005, The Astrophysical Journal, 618, 259
Meijerink, R., Spaans, M., & Israel, F. P. 2007, Astronomy and Astrophysics, 461, 793
Miao, Y., Mehringer, D. M., Kuan, Y.-J., & Snyder, L. E. 1995, ApJ, 445, L59
Mills, E. A. C., Butterfield, N., Ludovici, D. A., et al. 2015, ApJ, 805, 72
Mills, E. A. C., Güsten, R., Requena-Torres, M. A., & Morris, M. R. 2013, The Astrophysical Journal, 779, 47
Mills, E. A. C., & Morris, M. R. 2013, ApJ, 772, 105
Molinari, S., Bally, J., Noriega-Crespo, A., et al. 2011, ApJ, 735, L33
Moster, B. P., Naab, T., & White, S. D. M. 2013, MNRAS, 428, 3121
Olofsson, H., Eriksson, K., Gustafsson, B., & Carlstroem, U. 1993, ApJS, 87, 305
Ponti, G., Terrier, R., Goldwurm, A., Belanger, G., & Trap, G. 2010, ApJ, 714, 732
Ponti, G., Morris, M. R., Terrier, R., et al. 2015, MNRAS, 453, 172
Privon, G. C., Herrero-Illana, R., Evans, A. S., et al. 2015, arXiv.org, 1509.07512v1
Qin, S. L., Schilke, P., Rolffs, R., et al. 2011, Astronomy and Astrophysics, 530, L9
Riquelme, D., Amo-Baladron, M. A., Martin-Pintado, J., et al. 2010, ArXiv e-prints, arXiv:1008.1873
Rodríguez-Fernández, N. J., Martín-Pintado, J., & de Vicente, P. 2001, A&A, 377, 631
Saintonge, A., Kauffmann, G., Wang, J., et al. 2011, MNRAS, 415, 61
Saintonge, A., Lutz, D., Genzel, R., et al. 2013, ApJ, 778, 2
Sakamoto, K., Aalto, S., Evans, A. S., Wiedner, M. C., & Wilner, D. J. 2010, The Astrophysical Journal, 725, L228
Sandstrom, K. M., Leroy, A. K., Walter, F., et al. 2013, ApJ, 777, 5
Scoville, N., Sheth, K., Walter, F., et al. 2014, arXiv.org, 1412.5183v1
Serabyn, E., Lacy, J. H., & Achtermann, J. M. 1992, ApJ, 395, 166
Sjouwerman, L. O., Pihlström, Y. M., & Fish, V. L. 2010, ApJ, 710, L111
Snyder, L. E., Kuan, Y.-J., & Miao, Y. 1994, in Lecture Notes in Physics, Berlin Springer Verlag, Vol. 439, The Structure and Content of Molecular Clouds, ed. T. L. Wilson & K. J. Johnston, 187
Tacconi, L. J., Genzel, R., Neri, R., et al. 2010, Nature, 463, 781
Tacconi, L. J., Neri, R., Genzel, R., et al. 2013, ApJ, 768, 74
Tafalla, M., Santiago-García, J., Hacar, A., & Bachiller, R. 2010, A&A, 522, A91
Tanaka, K., Oka, T., Matsumura, S., Nagai, M., & Kamegai, K. 2011, ApJ, 743, L39
Terrier, R., Ponti, G., Bélanger, G., et al. 2010, ApJ, 719, 143
Usero, A., Leroy, A. K., Walter, F., et al. 2015, AJ, 150, 115
Vogel, S. N., Genzel, R., & Palmer, P. 1987, ApJ, 316, 243
Wilson, T. L. 1999, Reports on Progress in Physics, 62, 143
Wilson, T. L., & Rood, R. 1994, ARA&A, 32, 191
Wu, J., Evans, II, N. J., Gao, Y., et al. 2005, ApJ, 635, L173
Yusef-Zadeh, F., Cotton, W., Viti, S., Wardle, M., & Royster, M. 2013, ApJ, 764, L19
Yusef-Zadeh, F., Roberts, D. A., Goss, W. M., Frail, D. A., & Green, A. J. 1996, ApJ, 466, L25+
Ziurys, L. M., & Turner, B. E. 1986, Astrophysical Journal, 300, L19
Zylka, R., Guesten, R., Henkel, C., & Batrla, W. 1992, A&AS, 96, 525

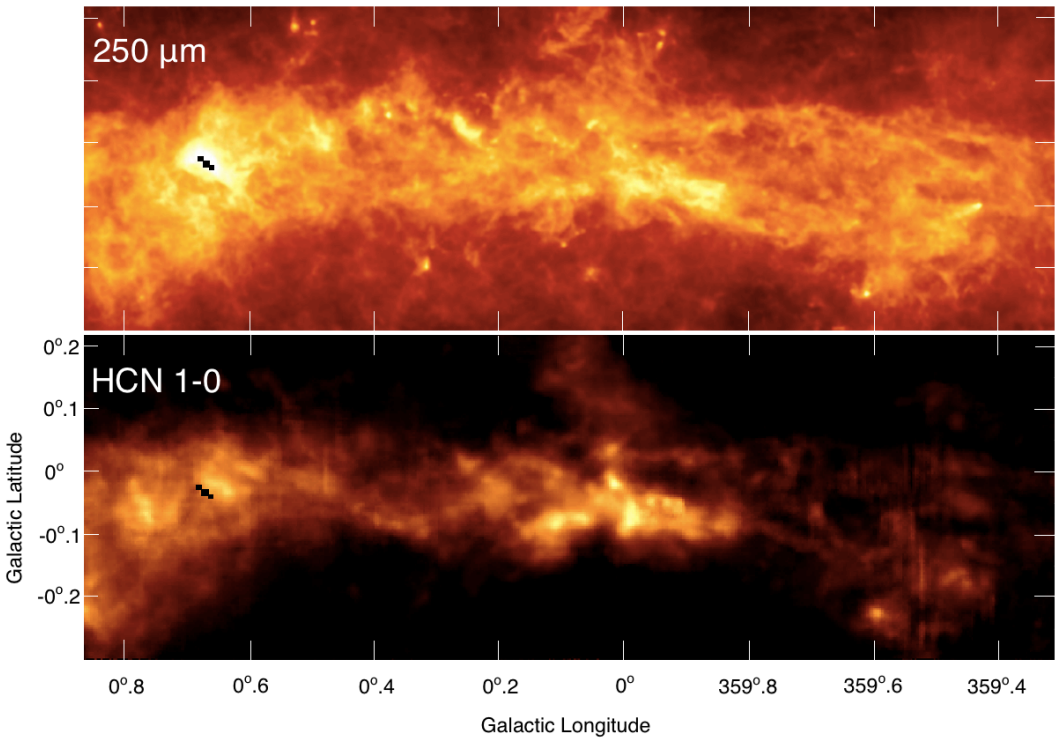

FIG. 1.— **Top:** A Herschel map of the 250 μm dust continuum from Molinari et al. (2011). Pixels at the center of Sgr B2 that are saturated in the Herschel data are masked out. **Bottom:** A map of the integrated line luminosity of HCN 1-0 in uncorrected antenna temperature T_A^*.

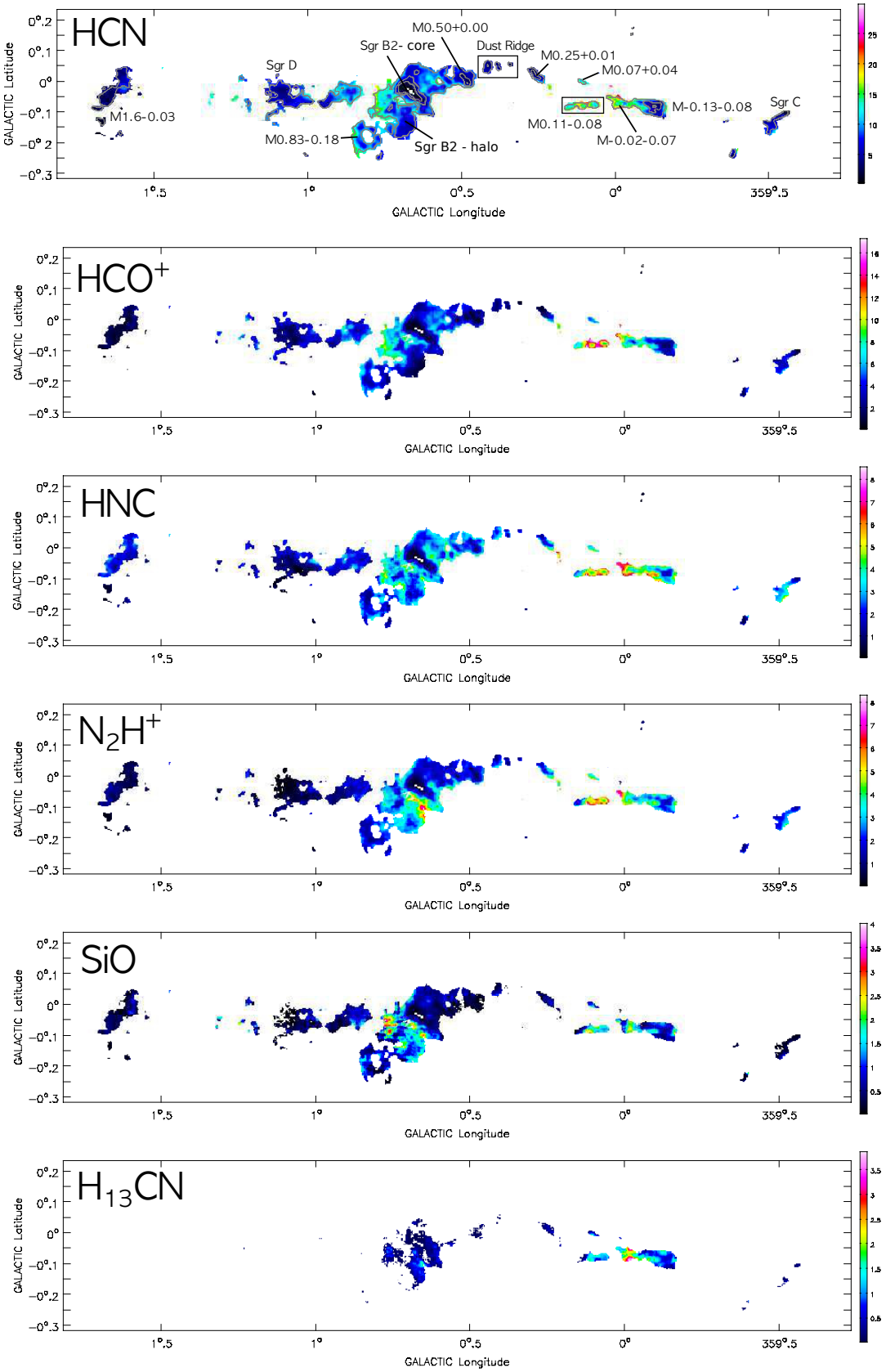

FIG. 2.— Maps of the molecular line luminosity to dense gas conversion factor. The units of the ratio shown are line luminosity in K km/s over the column density in units of 10^{22} cm^{-2}. The individual clouds studied in this analysis are identified in the first subfigure (HCN 1-0) which also shows contours of the column density for three levels: 8×10^{22}, 2×10^{23}, and 4×10^{23} cm^{-2}. For all of the maps, ratios are only computed where the column density is above a threshold of 7e22, and the molecular line is above a threshold of either 0.20 or 0.34 K km s^{-1}(see Section 2).

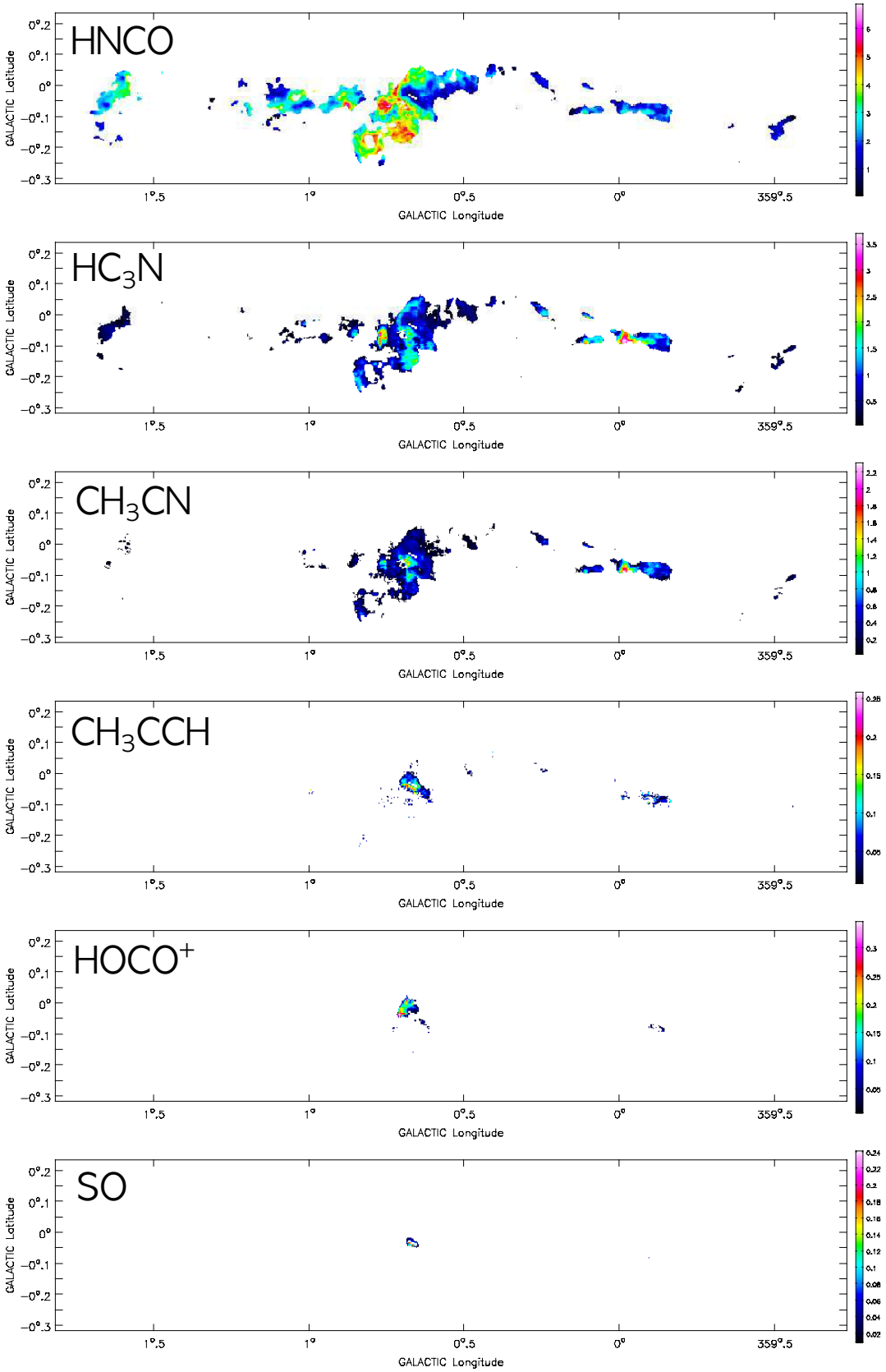

FIG. 2.— Continued

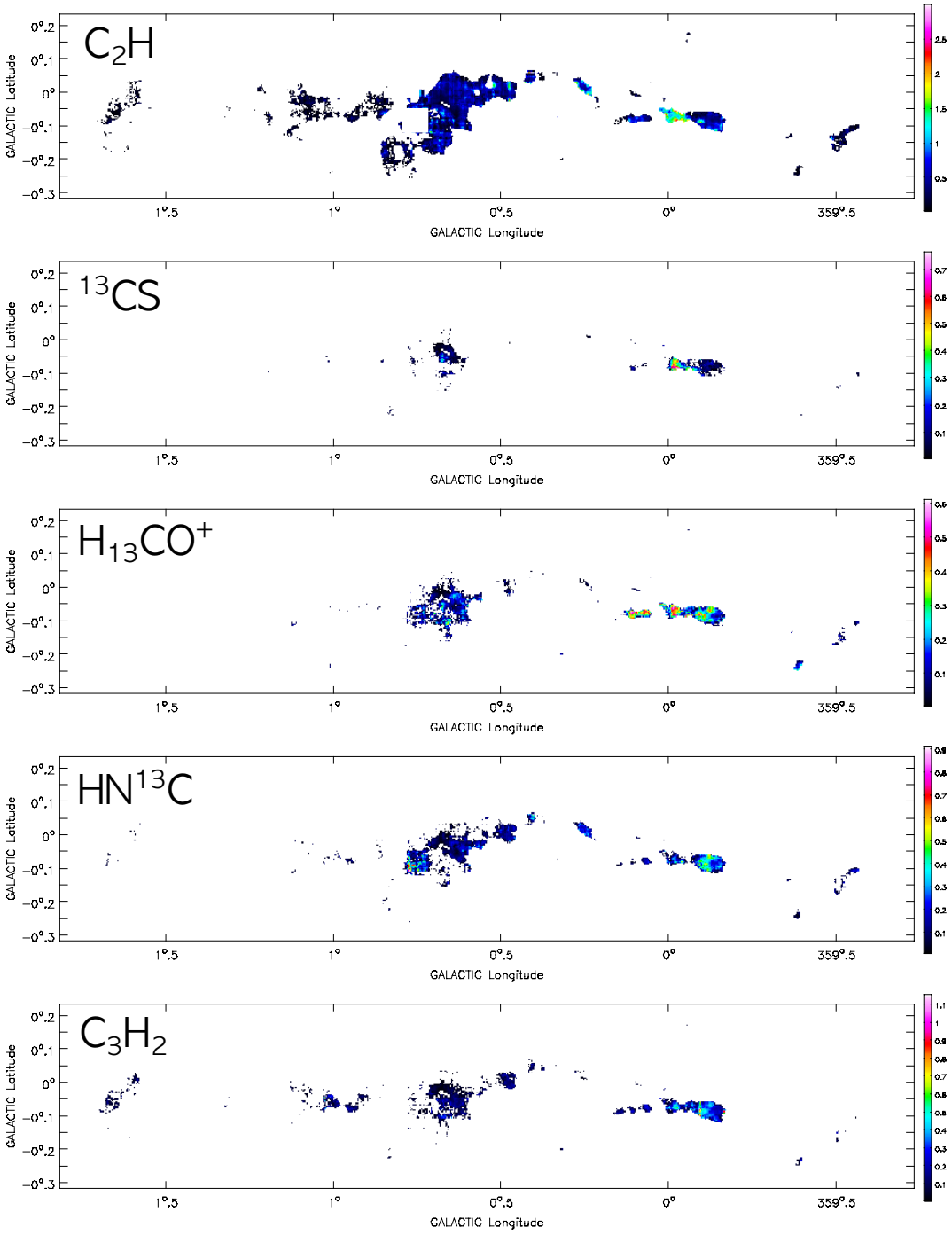

FIG. 2.— Continued

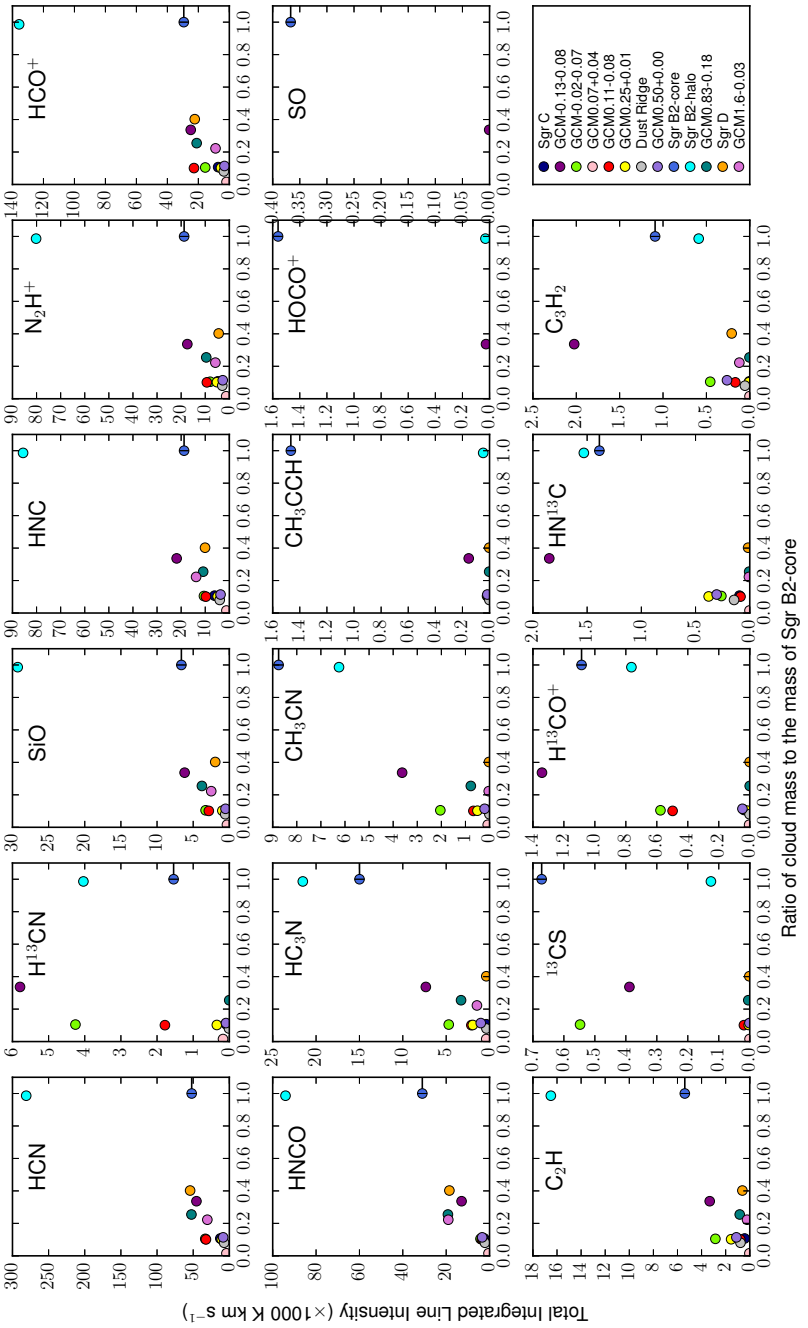

FIG. 3.— Plots of the total luminosity of HCN 1-0 and selected other lines ($H^{13}CN$,HNCO,HC_3N, and CH_3CN) compared to the total (dense) gas mass from the Herschel column density map, integrated over a sample of 13 Galactic center giant molecular clouds. The relevant uncertainties for this comparison are the errors in the relative calibrations across the molecular line and column density maps, and these are less than the size of the points plotted here. The mass of the Sgr B2 core is shown as a lower limit as the column density map of this source omits the brightest pixels at the peak of this cloud. Note that $^{12}C/^{13}C$ ratios should not be inferred from the values plotted here, as the ^{13}C isotopologues are weak enough to be below the detection limit in many parts of the cloud where the main isotopologue is detected, and this biases the cloud-averaged $^{12}C/^{13}C$ ratios to be greater than is actually observed.

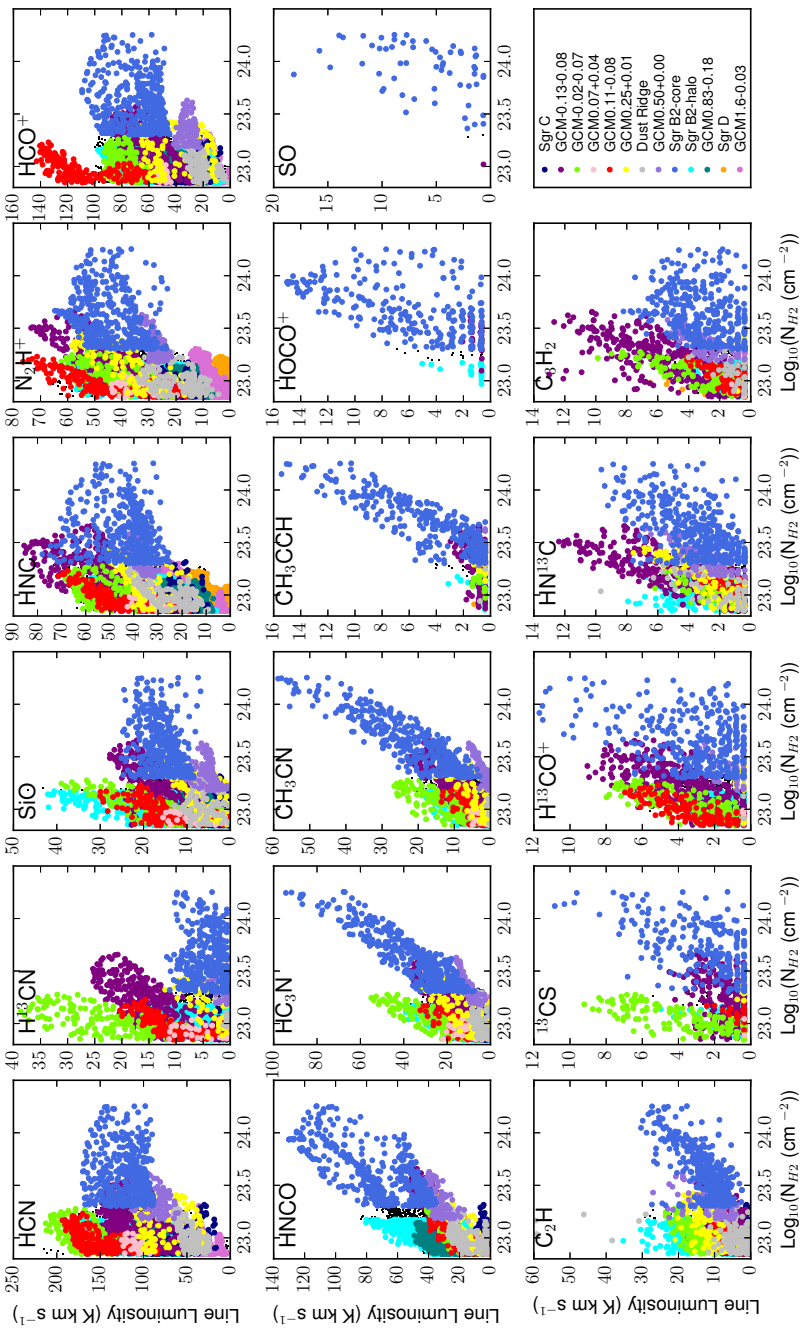

FIG. 4.— Plots of the luminosity of HCN 1-0 and all other 3 mm lines from Jones et al. (2012) compared to the base-10 logarithm of the Herschel column density map on a pixel-by-pixel basis. Pixels corresponding to the 13 Galactic center giant molecular clouds analyzed in this paper are colorized according to the legend at the bottom right. In order to better visualize the differences between individual sources and account for the large dynamic range in column density values, the column density is given as a logarithm– this is not motivated by any expected physical relationship between line brightness and the logarithm of the column density.

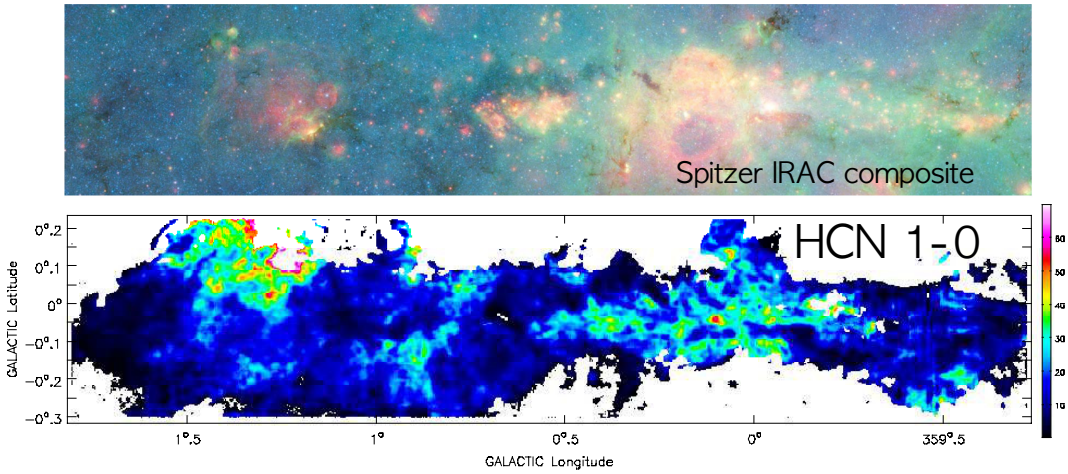

FIG. 5.— **Top:** A composite map of the infrared emission in the Galactic center from 3 to 8 microns, using Spitzer-IRAC. **Bottom:** A map of the HCN 1-0 luminosity to dense gas conversion factor. The units of the ratio shown are line luminosity in K km/s over the column density in units of 10^{22} cm^{-2}. The ratios is computed where the column density is above a threshold of $1{\times}10^{22}$ cm^{-2} and the HCN 1-0 intensity is above a threshold of 0.34 K km s^{-1}.

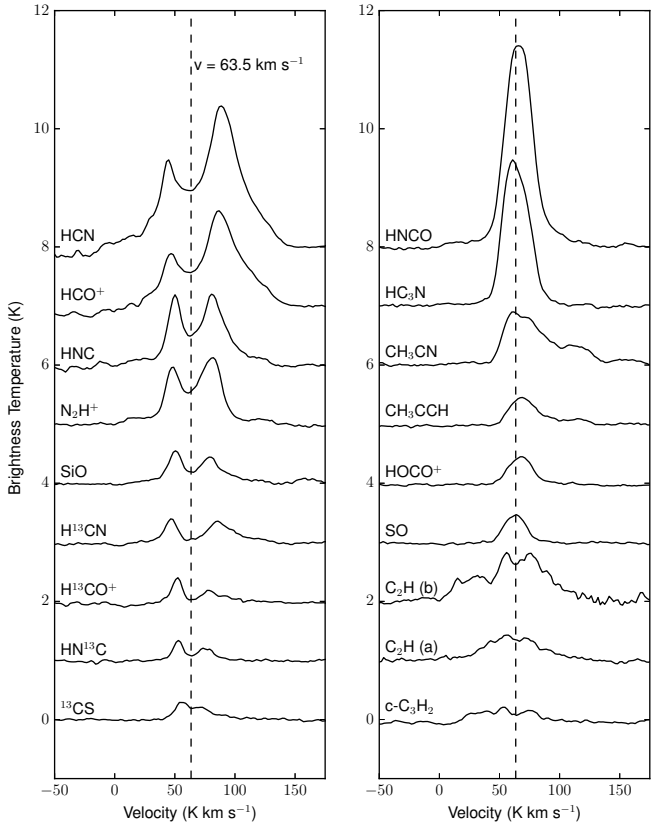

FIG. 6.— Average spectra of emission toward the core of the Sgr B2 cloud. All species whose ground (1-0) transitions are observed exhibit a distinctive two-peak morphology, characteristic of self-absorption around a central velocity of ∼64 km s^{-1}. Note that the signature of self-absorption is seen even in the 1-0 transitions of less abundant ^{13}C isotopologues. Self-absorption is also seen in the 2-1 transitions of ^{13}CS SiO, and possibly c-C_3H_2, however the (2_2-1_1) transition of SO appears largely unaffected, as do transitions with $J_{up} \geq 4$.